ARGONNE NATIONAL LABORATORY
Argonne, Illinois

DESIGN OF AN IONIZATION CHAMBER CAPABLE OF BROAD LINEAR RESPONSE

K.K. F.H.
Ken Krolik and F. Hornstra, Jr.
Accelerator Division
September 26, 1969

KK/FH-1

The ionization chamber is a device for collecting the ionized particles produced within it by means of an electric field. For moderate levels of ionization there seems to be no problem in obtaining meaningful and linear results using standard plate arrangements and precautions. However, when the number of ionizing particles becomes great enough to cause a sufficient current density within the chamber, the linearity of the chamber may fail for a number of reasons. The purpose of this design was to obtain linear response from an ion chamber to current densities of 6×10^{12} protons per sec - cm^2 ($\sim 1 \mu A/cm^2$).

First we had to investigate the causes of non-linearity during high levels of ionization. There seems to be two major causes for the loss of ionized particles within the ion chamber.

The first of these, is loss due to recombination. When positive and negative ions (or electrons) exist in the same region, there is a tendency

for them to recombine to form neutral molecules. The rate of recombination per unit volume can be described by the following expression:[1]

$$\frac{dn^+}{dt} = \frac{dn^-}{dt} = -\alpha n_+ n_-$$

where n_+ is the density of positive ions,

n_- is the density of negative ions,

α is the recombination constant.[2]

The fractional loss in saturation current due to recombination has been determined by Price for the parallel plate ion chamber.[3]

$$\left(\frac{\Delta I}{I}\right)_{Rec} = \frac{v_A \alpha n_+ n_- dx\, dy\, dz}{v_A N_o(x, y, z)\, dx\, dy\, dz} \qquad (1)$$

where v_A is the active volume of the chamber,

ΔI is the saturation current loss,

$N_o(x, y, z)$ is the number of ion pairs produced per unit volume per unit time.

$$n_-(x) = \frac{N_o x}{w_-} \qquad n_+(x) = \frac{N_o(d-x)}{w_+} \qquad (2)$$

where d is the plate spacing,

w_- is the negative ion drift velocity,

w_+ is the positive ion drift velocity.

Combining Equations (1) and (2) we arrive at the following expression:

$$\left(\frac{\Delta I}{I}\right)_{Rec} = \frac{\alpha N_o d^2}{6 w_+ w_-} \qquad (3)$$

We see from the last expression, that to keep the fractional loss of ion chamber current due to recombination as small as possible during high ion production, one must make a careful choice of the gas which fills the chamber so as to assure a low recombination constant, high ion drift velocities, and low ion production per ionizing particle. One might also note the effect of the plate spacing on the fractional recombination loss.

The second major source of ion current loss in the parallel plate ion chamber is described as diffusion loss. Diffusion loss occurs when charges move in directions not with the electric field. This situation could occur when the ion density gradient is not in agreement with that of the electric field. Hence some of the charges may be lost from the sensitive volume of the chamber.

The fractional loss of ion chamber current due to diffusion phenomenon is given by Rossi and Staub[4] for the parallel plate ionization chamber.

$$\left(\frac{\Delta I}{I}\right)_{Diff} = \frac{2.5 \times 10^{-2} (E^{+} + E^{-})}{V_o} \qquad (4)$$

where E is the ratio of mean energy of ions with and without the electric field present,

V_o is the potential across the ion chamber plates.

Since E is approximately one for heavy positive and negative ions, the diffusion loss becomes important when small voltages exist on the chamber and the negative ions are free electrons.

A third phenomenon, called attachment, may occur when atoms with a positive electron affinity are present within the chamber. Free electrons have a probability of attachment to these atoms, causing the formation of heavy negative ions; negative ions have a very slow transit time in crossing the chamber compared to that of free electrons. Hence, when a large number of electrons attach themselves to neutral atoms in a chamber with a high ion density, the recombination loss will increase due to the considerable decrease in negative ion drift velocity as indicated in Eq. (3).

Of primary concern then to the construction of linear chamber for use in high density ionizing particles, is minimizing the number of ion pairs produced per ionizing particle to the least possible number. This would mean obtaining the lowest possible energy loss per unit distance traveled by each particle. Bethe and Livingston[5] have derived the relation for obtaining the energy loss per unit distance for a proton passing through a gas within the limits of the relation.

$$\frac{dE}{dx} = \frac{4\pi(ez)^2 e^2 N}{mv^2} Z\left[\ln\left(\frac{2mv^2}{I}\right) - \ln(1-\beta^2) - \beta^2\right] \qquad (5)$$

where ez is the charge of a proton,
e is the charge of an electron,
Z is the atomic number,
m is the mass of an electron,
c is the velocity of light,
v is the velocity of the ionizing particles,

I is the average ionization energy,

N is the number of atoms per cm^3 of gas,

β is v/c.

Since for a particular high energy particle, the average ionization energy does not vary greatly from gas to gas, the Atomic number of the gas becomes very important if we are to minimize the ion pair production.

With these ideas in mind, we proceeded to design an ion chamber. For our purposes we were to build a chamber capable of measuring the intensity of a high energy proton beam with no more than one percent saturation or diffusion loss. The range of the measured beam current density was to be from 6×10^9 protons per sec - cm^2 ($\sim$1 nA/cm^2) to 6×10^{12} protons per sec - cm^2 ($\sim 1 \mu A/cm^2$).

The chamber was constructed so that the proton beam is perpendicular to the plates of the ion chamber and passes through the middle of each plate. In this way, the material the proton beam must pass through is held to a few mg/cm^2. The ion chamber plates were constructed of 0.8 mil aluminum, and five inches in diameter. The plates themselves are completely enclosed with 2 mil mylar windows to insure low beam loss. For structural considerations and practical purposes, the gas pressure of the chamber is kept at a slight positive value with a small leak installed to insure the purity of the gas. One should note from Figures 1A and 1B, the presence of the guard rings in the ion chamber. The use of these rings assures that leakage

current crossing the insulating spacers will not reach the signal electrode. At the small plate spacings of our design, this precaution becomes absolutely necessary.

Helium was chosen as the gas for our ion chamber for the following reasons:

1. A low atomic number to keep the ion density as low as possible.
2. A negative electron affinity to limit the formation of heavy negative ions.
3. A high negative ion (electron) drift velocity for a given electric field strength (mobility).
4. A high positive ion mobility.
5. Safety, ease of handling, and availability.

In the construction and testing of the chamber, we found that in an atmosphere of pure helium, the breakdown voltage of the chamber was greatly decreased over that experienced in air. The final plate spacing was set at 3.5 mm as a compromise between ease of fabrication and performance.

Below are the calculations for an ion chamber having the following specifications:

1.	Gas (atmosphere)	- Helium
2.	Plate spacing	- 3.5 mm
3.	Gas pressure (P)	- 760 + mm (Hg)

4.	Operating voltage	- 600 V dc
5.	Electric field (E)	- 1700 V/cm
6.	E/P	- 2.25
7.	Particles to be measured	- 10-11.5 BeV protons

Calculating the energy loss of the protons in the chamber using Eq. (5) we obtain:

$$\frac{de}{dx} = \frac{4\pi(ez)^2 e^2 NZ}{mv^2} \left[\ln\left(\frac{2mv^2}{I}\right) - \ln(1-B^2) - B^2 \right]$$

where $ez = 4.813 \times 10^{-10}$ st coul,

$e = -4.813 \times 10^{-10}$ st coul,

$Z = 2$,

$m = 9.11 \times 10^{-28}$ grams,

$c = 2.99 \times 10^{+10}$ cm/sec,

$v = 0.999\,c$,

$I = 27.8$ eV (44.5×10^{12} ergs), (Ref. 6)

$N = 25.2 \times 10^{18}$ molecules/cm^3,

$B^2 = 0.99126$ (10 BeV protons),

$B^2 = 0.99333$ (11.5 BeV protons).

Solving for 10 BeV protons

$$\frac{de}{dx} = 5.82 \times 10^{-10} \text{ erg/cm (10 BeV protons)}$$

The number of ion pairs produced per unit distances is:

$$S = 13.1 \frac{\text{ion pair}}{\text{cm proton}} \quad \text{(10 BeV protons)}$$

Solving again for 11.5 BeV protons

$$\frac{dE}{dx} = 5.98 \times 10^{-10} \text{ ergs/cm} \qquad (11.5 \text{ BeV})$$

$$S = 13.4 \frac{\text{ion pair}}{\text{cm proton}} \qquad (11.5 \text{ BeV})$$

Solving for the recombination losses during high current density

$$\left(\frac{\Delta I}{I}\right)_{Rec} = \frac{a M_o d^2}{6 W_+ W_-}$$

where $a = 1.7 \times 10^{-8} \text{ cm}^3/\text{sec}$, (Ref. 2)

$W_+ = 2.0 \times 10^4 \text{ cm/sec}$, (Fig. 2)

$W_- = 1.4 \times 10^6 \text{ cm/sec}$, (Figs. 3 and 4)

$M_o = 7.95 \times 10^{13} \frac{\text{ion pair}}{\text{cm}^3 - \text{sec}}$, (Assuming a current density of 6×10^{12} protons/sec-cm^2)

$$\left(\frac{\Delta I}{I}\right)_{Rec} = 1.0 \times 10^{-6},$$

$$\left(\frac{\Delta I}{I}\right)_{Rec} = 0.00010\%.$$

Solving for the diffusion loss

$$\left(\frac{\Delta I}{I}\right)_{Diff} = \frac{2.5 \times 10^{-2} (E^+ + E^-)}{V_o}$$

where $E^+ \cong 1$,

$E^- = 120$, (Fig. 5)

$V_o = 600 \text{ V}$,

$$\left(\frac{\Delta I}{I}\right)_{Diff} = 0.005,$$

$$\left(\frac{\Delta I}{I}\right)_{Diff} = 0.5\%.$$

Examining the amount of charge per proton (sensitivity) we will collect from the ion chamber:

Sensitivity

Case 1 (11.5 BeV) - 1.51×10^{-18} coul/proton

Case 2 (10.0 BeV) - 1.47×10^{-18} coul/proton

In any chamber there may be an increased output due to secondary collisions within the atmosphere of the chamber. This can come about when a light ion can gain enough energy from the electric field to ionize other atoms.

Finding the average energy of an electron $\overline{E}_e$:

$$\overline{E}_e = E^- \left(\frac{3KT}{2}\right)$$

where K = Boltzman's constant,

T = the temperature in degrees Kelvin,

E^- = the ratio of the average energy of the ions in an electric field to the thermal agitation energy (120 for E/p of 2.25),

$\overline{E}_e = 120\ (3.8 \times 10^{-2}\ eV)$,

$\overline{E}_e = 4.5$ eV.

The minimum ionization energy for Helium is 24.6 eV.

Finding the increase in output current due to secondary collisions using Townsend's first ionization coefficient[7]

$$I = I_o e^{ad}$$

where I = the output current,

I_o = the output current in the zero multiplication region,

a = Townsend's first ionization coefficient,

d = the plate spacing.

Therefore for $E/p = 2.25$

$$a/p = 10^{-7} \qquad \text{(Ref. 8)}$$

$$a = 10^{-4}$$

$$\frac{I}{I_o} = e^{10^{-4}(.35)}$$

$$\frac{I}{I_o} \cong 1$$

Hence no multiplication.

The completed chamber is connected to the circuit shown in Figure 6. An explanation of the circuit is as follows. Ion chamber current is integrated by the 2 mf capacitor with both field effect transistors (FETs) in the OFF state. The FETs are controlled by logic circuits according to the purpose of the experiment. FET 1 has the purpose of shorting out unwanted portions of the proton beam spill while FET 2 discharges the integrating capacitor. The voltage level on the integrating capacitor is directly proportional to the

number of protons passing through the ion chamber (Fig. 7). Changing this analog output to a digital output, one can directly read the number of protons passing through the chamber. By using a second voltage follower circuit we may obtain a profile of the intensity of the ionizing proton beam as a function of time. This is done by obtaining a differential output of the two voltage follower circuits (Fig. 8).

At the writing of this paper, eight ion chambers have been constructed and in operation for several months. Initial calibration was obtained by adjusting the sensitivity of the ion chamber readout to correspond to that of SEM 1 (± 5% absolute) at a given beam current. A comparison of the two devices is shown in Fig. 9. It should be noted that the SEM 1 readout has an inherent positive offset, resulting in high readings at low beam currents. This comparison confirms chamber linearity for several chamber potentials.

Although the ion chamber was not meant to have an absolute calibration, calculated and experimental sensitivities are in close agreement. Final chamber readout sensitivity was set at 1.50×10^{-18} coul/proton, as calibrated from SEM 1, while calculated sensitivity is 1.51×10^{-18} coul/proton for 11.5 BeV protons. All results were obtained using ultra-high purity helium within the chamber, while calculations were based on normal atmospheric conditions (760 mm, 22°C). Typical pressure and temperature variations encountered by the chamber should affect its sensitivity by no more than 3%.

As a final thought, since the chamber is operating well within its linear range, as indicated by its insensitivity to applied voltage (Fig. 9), it can be assumed that the chamber will operate lineally at considerably higher beam current densities. Further tests are being planned to confirm this assumption.

The help of D. Suddeth, B. Scherr, R. Seglem, J. Seeman, and J. Davis in the construction and installation of these devices is gratefully acknowledged.

KK/FH:paw

Distribution:

J. J. Livingood
E. N. Pettitt (2 copies)
W. J. Ramler
L. G. Hyman
R. A. Schluter
G. J. Marmer
Group Leaders
L. C. Teng (NAL)
R. L. Martin
D. S. Manson
R. J. Jones
T. Groves
L. Strom
T. Romanowski
V. Telegdi
E-215
E-172
E-226
E-209
E-206
D. Suddeth
B. Scherr (NAL)
R. Nielsen
J. Seeman
R. Seglem
D. Geigner
F. Brandeberry
J. Davis

References

1. William J. Price, Nuclear Radiation Detection (1958), pages 68-70.

2. J. Craggs and J. Mech, Electrical Breakdown of Gases (1953).

3. William J. Price, Nuclear Radiation Detection (1958), pages 71-72.

4. B. Rossi and H. Staub, Ionization Chambers and Counters (1949), pages 27-29.

5. H. Bethe and M. S. Livingston, Review of Modern Physics, 9, 263 (1937).

6. J. Craggs and J. Mech, Electrical Breakdown of Gases (1953), page 16.

7. ibid., pages 52-66.

8. ibid., pages 63-64.

9. A. Engel, Ionized Gases (1965), page 121.

10. J. Craggs and J. Mech, Electrical Breakdown of Gases (1953), page 39.

11. B. Rossi and H. Staub, Ionization Chambers and Counters (1947), page 10.

12. ibid., page 16.

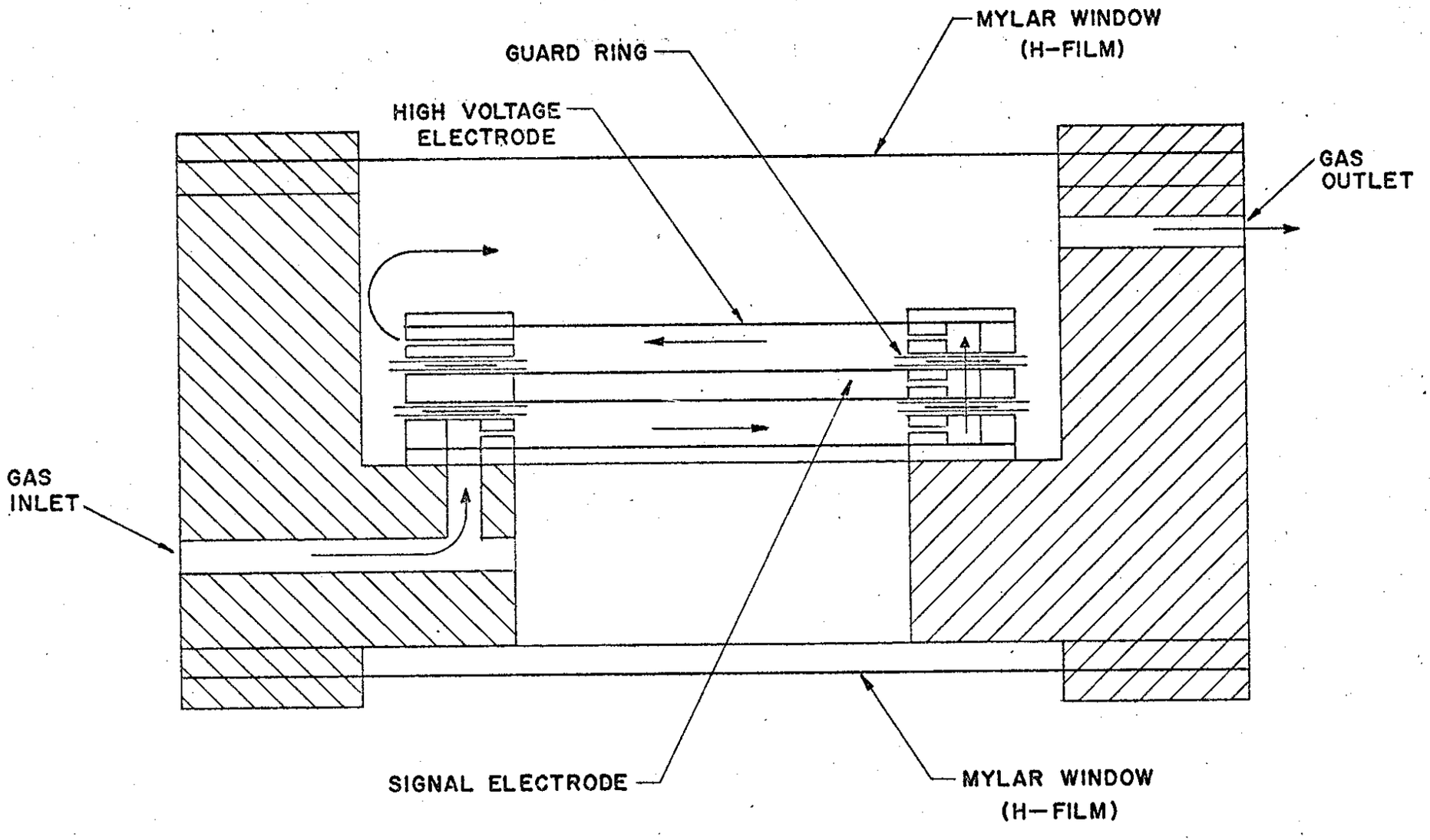

FIG. 1A — ION CHAMBER CROSS SECTION

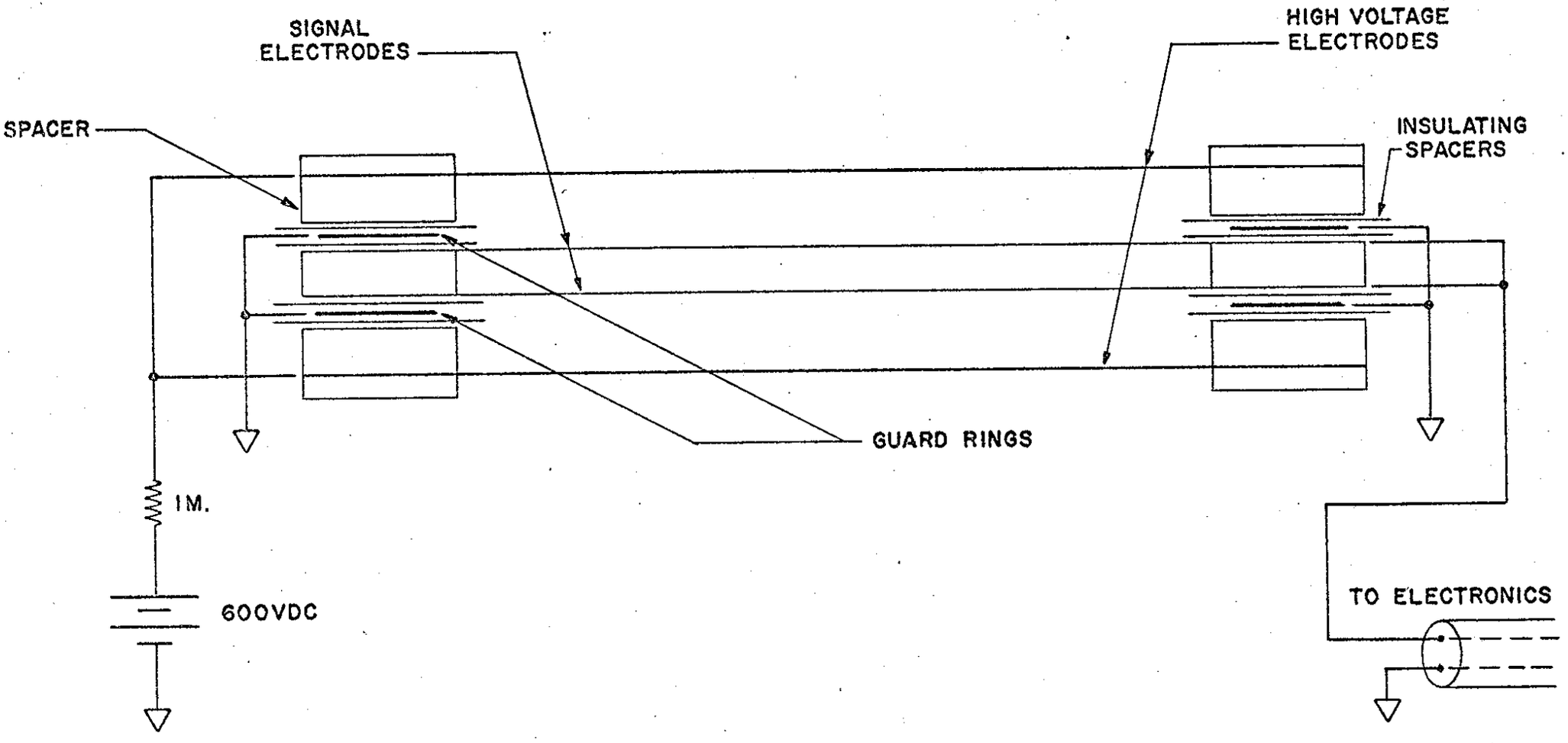

FIG. 1B — ION CHAMBER PLATE ARRANGEMENT AND ELECTRICAL CONNECTIONS

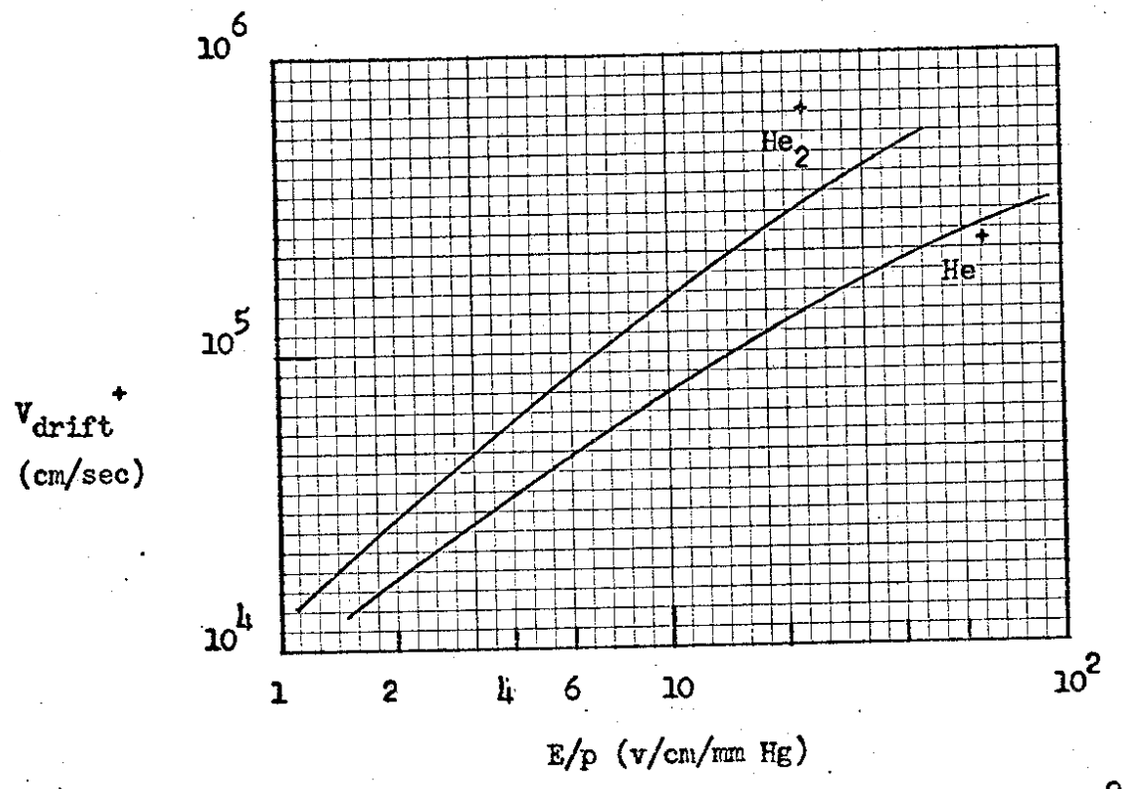

Fig.2 - Positive ion drift velocity in Helium [9]

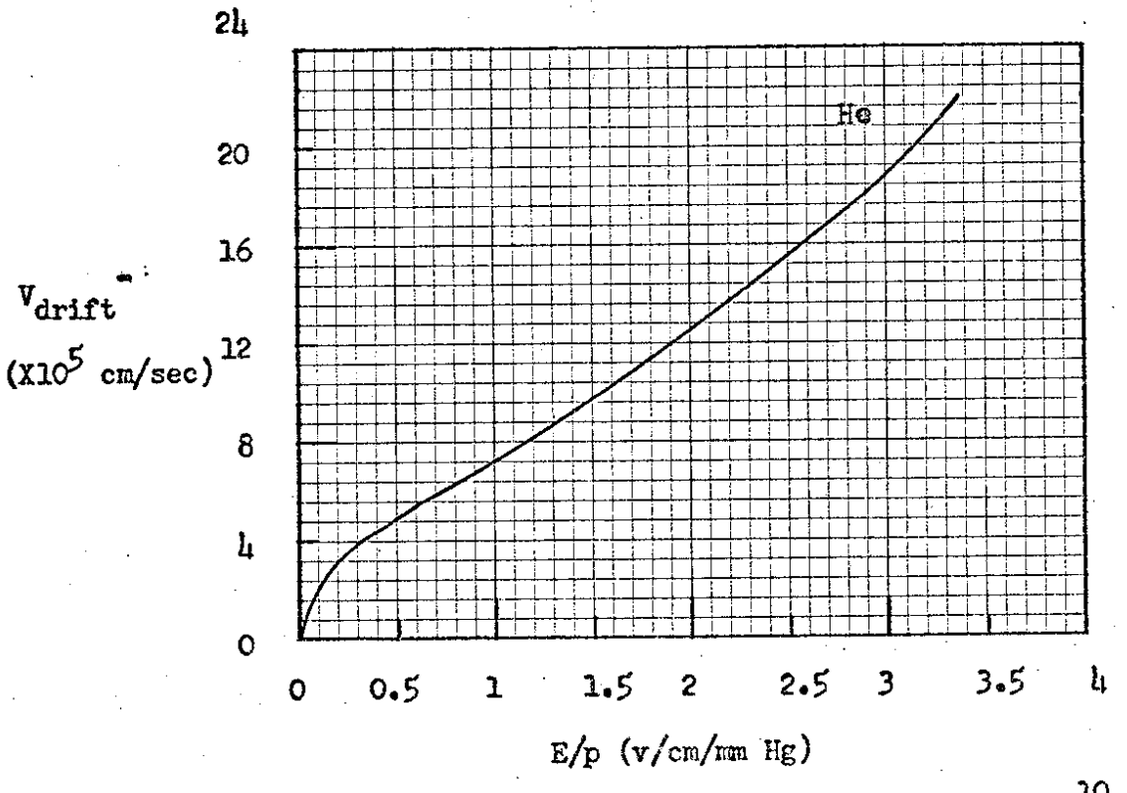

Fig.3 - Electron drift velocities in Helium [10]

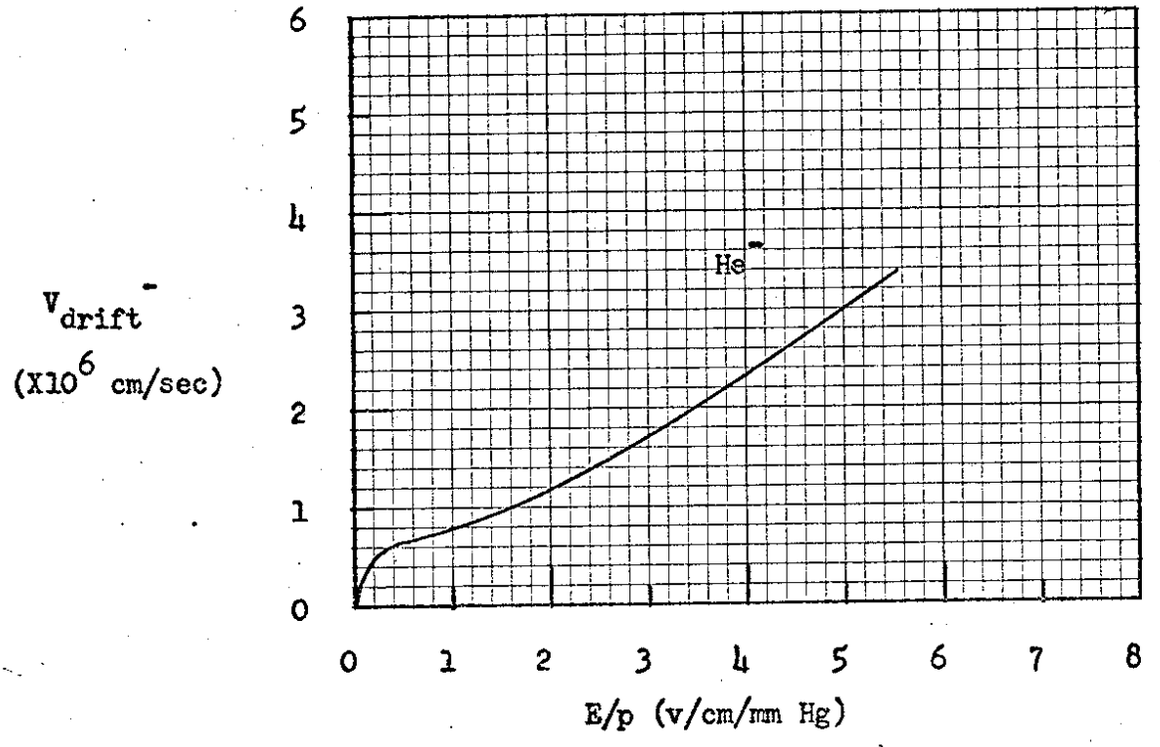

Fig. 4 - Electron drift velocities in Helium [11]

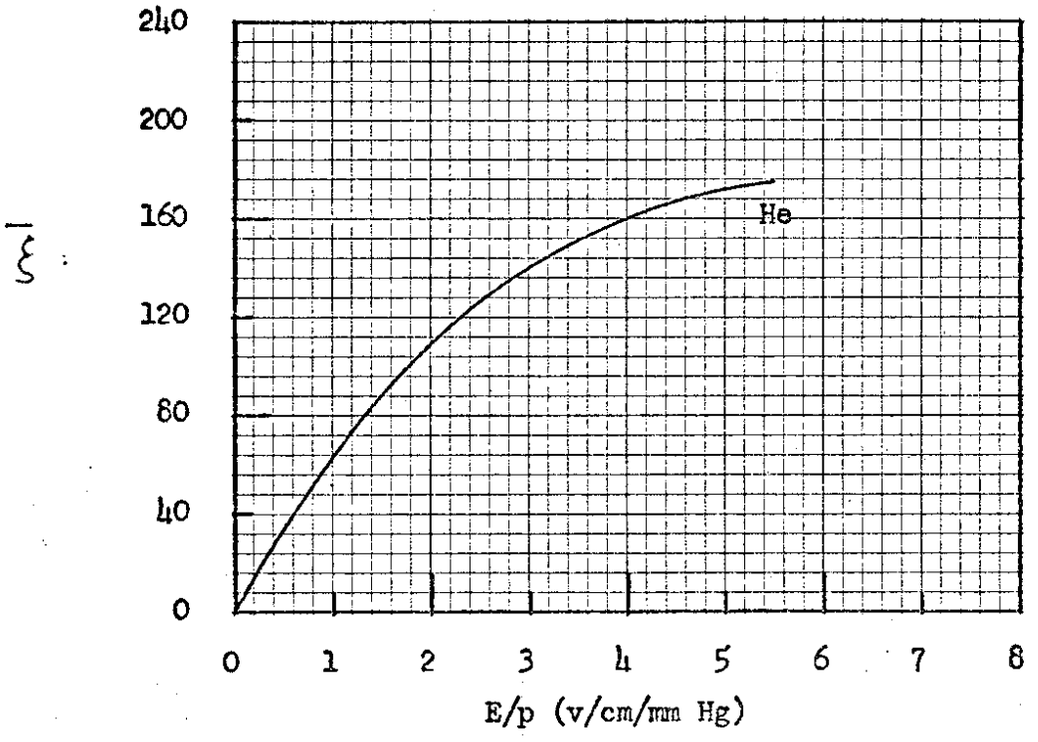

Fig. 5 - Mean agitation energy of electrons as a function of E/p for Helium [12]

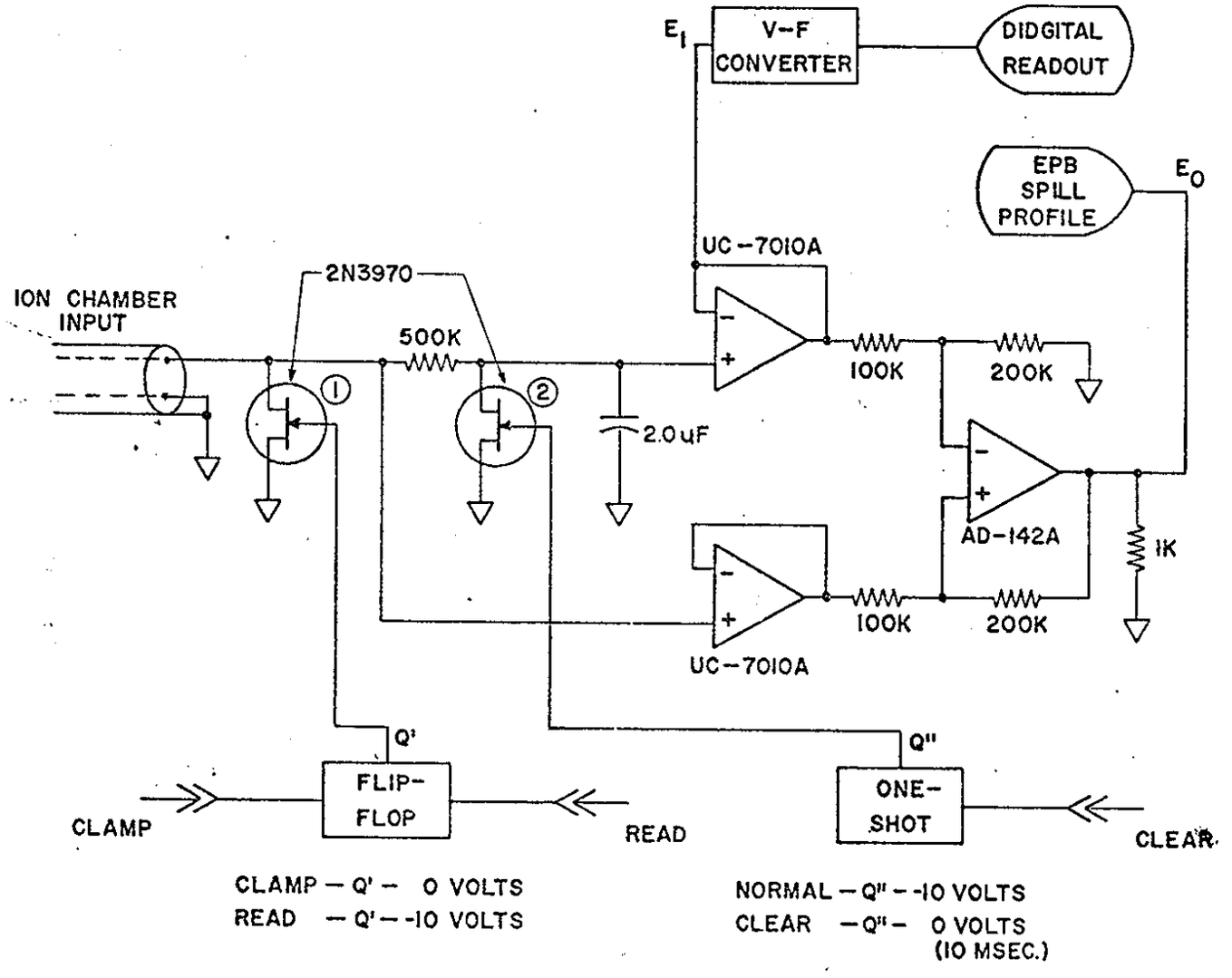

FIG. 6 — ION CHAMBER ELECTRONICS

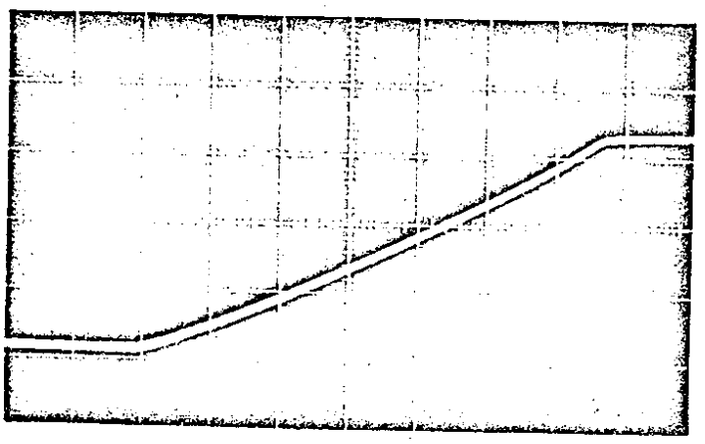

V - 0.2 v/cm

H - 100ms/cm

Fig.7 - Analog Voltage Output (E_1)

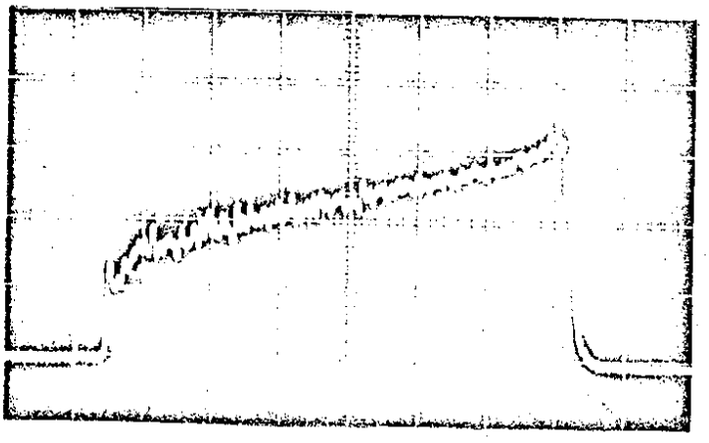

V - 0.2 v/cm

H - 100ms/cm

Fig.8 - EPB Spill Profile (E_o)

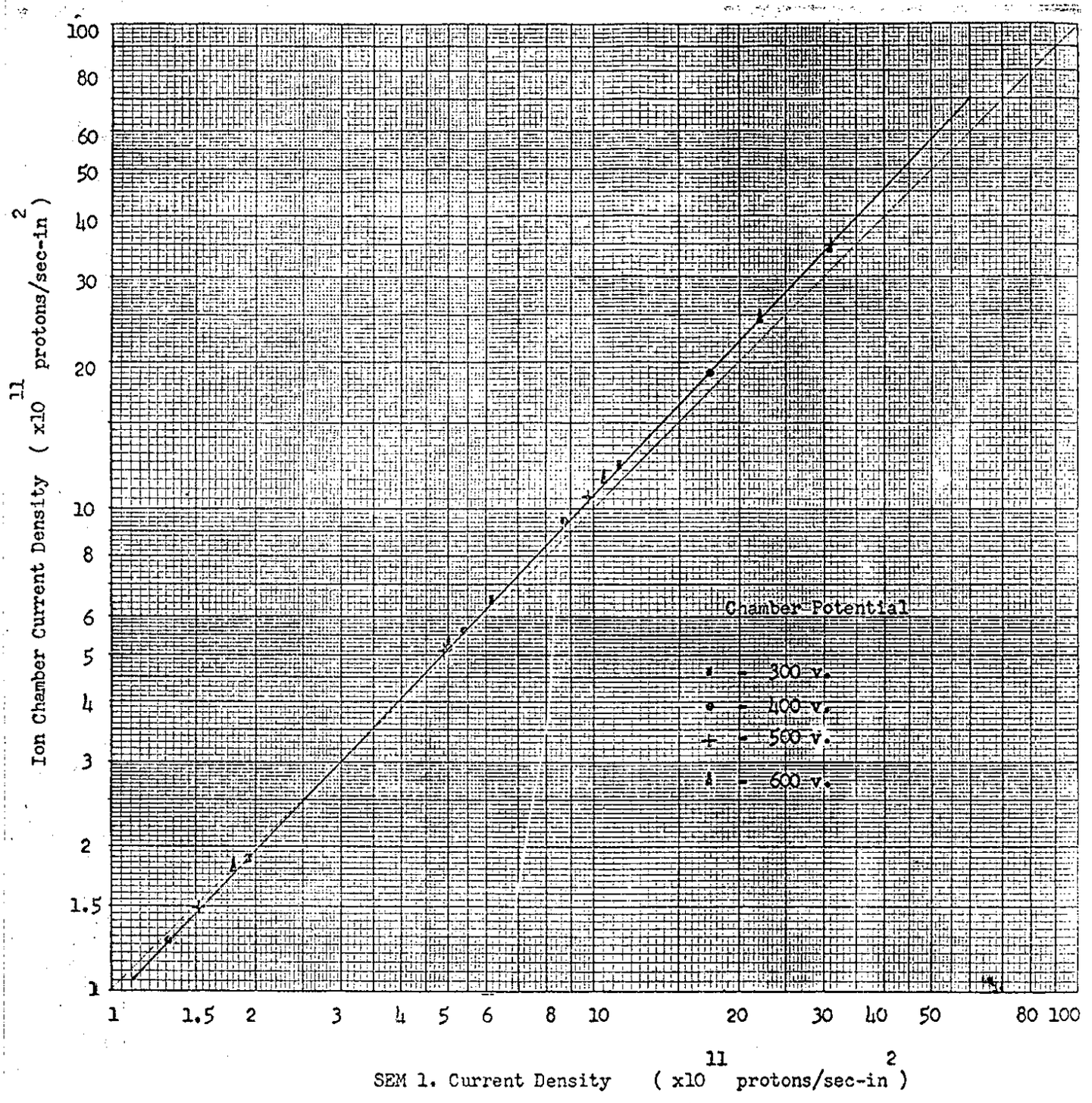

Fig.9 - SEM 1. - Ion Chamber Comparison